Water Practice & Technology Vol 16 No 2
doi: 10.2166/wpt.2020.117

Removal of methylene blue from aqueous solutions by adsorption on amorphous silicon dioxide from rice husks

O. D. Arefieva[a,b,*], L. A. Zemnukhova[b], V. A. Gorlova[a] and M. A. Tsvetnov[a]

[a] Far Eastern Federal University, Vladivostok, Russian Federation

[b] Institute of Chemistry, Far-Eastern Branch, Russian Academy of Sciences, Vladivostok, Russian Federation

*Corresponding author. E-mail: arefeva.od@dvfu.ru

Abstract

This study shows the effect of conditions on methylene blue sorption from aqueous solutions using amorphous silicon dioxide obtained from rice husk by oxidative roasting with and without pre-treatment with 0.1 M HCl. Adsorption activity for methylene blue increases with increasing pH, reaching its maximum above the point of zero charge. Thermodynamic parameter values ($\Delta G_{298} > 0$, $\Delta H < 0$, $\Delta S > 0$) indicate that methylene blue adsorption is exothermic and occurs with an increase in molecular mobility in the adsorption layer. The process is described by the Freundlich and Dubinin-Astakhov equations, which indicates that it is determined by both electrostatic interaction with active centers on the surface and the volumetric filling of micropores.

Key words: adsorption, kinetics, methylene blue, rice husk, silica, thermodynamics

Highlights

- Characterization of the rice husk ash with different silica contents.
- The study of the effect of conditions on the sorption of methylene blue from aqueous solutions.
- The mechanism of adsorption of methylene blue by silicon-containing sorbents from rice husk.

INTRODUCTION

Dyes with intense adsorption bands in the ultraviolet and visible regions of the spectrum are commonly used to assess the adsorption capacity of adsorbents. One such is methylene blue (MB) (Balykin *et al.* 2004). The MB sorption activity of materials is determined by various spectrophotometric methods that differ in sorbent:solution ratio and wavelength. The sorbent:solution ratios are typically - 1:10, 1:100, 1:250, 1:500, and/or 1:1,000, and the wavelength varies from 660 to 690 nm (Selyutin *et al.* 2013; P'yanova *et al.* 2017). In addition to spectrophotometric methods, the sorption activity of clays is often determined using a titrimetric method based on titration of an aqueous suspension with an MB solution. No unified method for determining the MB sorption activity for various materials has yet been developed, however.

The behavior of MB in solution and the adsorption capacities of materials depend on many factors: composition, physicochemical properties, adsorbent mass, initial dye concentration, solution pH, contact time between adsorbent and dye, and temperature. All of these make it difficult to compare the quality of the sorbents described by different researchers.

MB sorption is influenced significantly by the adsorbent dose with the remaining conditions unchanged. For example, the maximum MB removal (82.47%) by pomegranate peel was achieved with a biosorbent content of 0.08 g in 100 ml of solution. Further addition of the sorbent had no significant effect (Jawad *et al.* 2018). When extracting MB from aqueous solution using bone charcoal as

Water Practice & Technology Vol 16 No 2
doi: 10.2166/wpt.2020.117

the sorbent, a dosage increase from 0.3 to 10 g in 50 ml of solution led to a decrease in adsorptive capacity (Ghanizadeh & Asgari 2011).

Solution pH affects adsorption efficiency significantly, regulating the degree of ionization of the adsorbate's functional groups (Singh *et al.* 2017) and the surface charge of the sorbent (Corda & Kini 2018). A number of works (Dŏgan *et al.* 2004; Dŏgan *et al.* 2009; Liu *et al.* 2012; Mulugeta & Lelisa 2014; Jia *et al.* 2017; Tamimi *et al.* 2018) report that MB adsorption is higher in an alkaline medium, and decreases in an acidic medium.

An important parameter is adsorbent contact time with the dye solution. As dye concentration increases, longer contact is required to reach equilibrium. For example, Jawad *et al.* (2018) showed that 50 mg/L of MB took about 120 min to reach adsorption equilibrium on pomegranate (*Punica granatum*) peel, while 300 mg-MB/L required almost 390 min. Pseudo-first and pseudo-second order models describe the kinetics of sorption onto sorbents of different nature, but, in this case, they obey principally the pseudo-second order equation (Vieira *et al.* 2009; Rafatullah *et al.* 2010; Soldatkina & Zavrichko 2018; Van *et al.* 2018).

Temperature is also important, and it has been shown that MB adsorption at temperatures between 293 and 333 K is an endothermic process and spontaneous in character (Liu *et al.* 2012; Tamimi *et al.* 2018; Lakkaboyana *et al.* 2019).

Mulugeta & Lelisa (2014) and Van *et al.* (2018) both report studies of the effect of initial MB concentration on its adsorption by dry, untreated *Parthenium hystrophorous* biomass and activated carbon from coconut shells. The studies show that the proportion of adsorption increases to a certain value, associated with an increase in surface area and the presence of a large number of adsorption sites. Then, as the concentration increases further, the number of active sites available becomes smaller, and the number are too few to remove MB, because of which adsorption capacity decreases. A number of studies (Djilani *et al.* 2015; Corda & Kini 2018; Jawad *et al.* 2018; Mouni *et al.* 2018; Soldatkina & Zavrichko 2018) have shown that the MB sorption isotherm on various sorbents – e.g. pomegranate (*Punica granatum*) peel, activated carbons from different sources, corn stalks modified by cetylpyridinium bromide, kaolin, etc – is best described by the Langmuir model.

Today, many researchers are attracted by cheap raw materials as sorbent sources. Rafatullah *et al.* (2010) considered the MB adsorption capacity of inexpensive materials – natural materials, biomass, industrial and agricultural wastes – in their review, and showed that they are effective and can be used instead of commercial activated carbons for MB removal from aqueous solutions.

About 150 million tonnes of rice husk (RH), a by-product of rice production, are produced globally annually. The maximum value of commercially available rice husk is approximately 0.025 USD kg^{-1}. Since the main components of RH are carbon and silica (15 to 22% SiO_2), it has potential for adsorbent production (Rafatullah *et al.* 2010). RH ash is one promising material, and, depending on the process used, silica of various qualities can be obtained from it, including 'black ash' (SiO_2 content 36 to 88%) with a yield of between 36 and 44%, and 'white ash' (SiO_2 90 to 99.99%) with 9 to 21% yield (Sergienko *et al.* 2004).

There is no comparative information on the effect of the conditions for MB removal from aqueous solutions on the sorption capacity indicators of RH ash with different silica contents in the literature. The purpose of this work was to study the effect of conditions on MB sorption from aqueous solution using RH-derived amorphous silicon dioxide.

METHODS

Sample development

RH was collected from a mill in Vietnam and meshed (~8 mesh) to remove tiny fractions (bran siftings, dust). It was then washed in distilled water and air dried, before being ashed at 300 °C to remove

Water Practice & Technology Vol 16 No 2
doi: 10.2166/wpt.2020.117

volatiles. After ashing, the material was subjected to oxidative roasting for 3 hours in a WiseTherm muffle furnace (DAIHAN, South Korea) at 650 °C. Finally, it was ground to a fine (gray) powder, referred to below as RH-1. RH-1 yield was 10.3%.

A portion of the meshed RH was hydrolyzed using 1 mol L^{-1} HCl heated to 90°C for an hour in a reactor. The temperature was controlled using an EKT Hei Con thermocouple (Heidolph, Germany). The solid:liquid mass ratio was 1:13, and the residue was filtered using synthetic fabric to 15 μm and air dried. After, the process was the same as that used to produce RH-1 – oxidative roasting in the muffle furnace for 3 hours at 650 °C followed by grinding to a fine (white) powder, referred to below as RH-2. RH-2 yield was 9.1%.

To study their sorption properties, both RH-1 and RH-2 were meshed (16 × 60 mesh) and dried at 105 °C to constant mass.

Sample characterization

The samples' silicon content was determined gravimetrically (GOST 9428-73 1993), while an atomic absorption spectrometer AA-780 (Shimadzu, Japan) was used to determine the elemental composition of impurities. X-ray diffraction was performed using a D8 ADVANCE diffractometer (Bruker, Germany) and CuKα-radiation. Infrared absorption spectra in the range 400 to 4,000 cm^{-1} in potassium bromide were recorded with Vertex 70 (Bruker, Germany), to determine the samples' functional groups.

Adsorption studies

The sorption studies were performed at a fixed temperature of 293 K. 0.004 g sorbent samples were placed in glass-stoppered, dry, conical flasks and 10 ml MB solution was added. The flask samples were mixed in a Unimax 1010 (Heidolph, Germany) shaker for 30 minutes, before being centrifuged for 15 minutes. The residual MB content was analyzed using visible spectrophotometry (UNICO-1201, United Products & Instruments Inc., USA) at a filtered wavelength (λ) of 660 nm.

All experiments were performed at least in triplicate. The results are the average of three independent measurements along with the standard deviation (SD) showing 95% confidence level.

The removal efficiency (%) or MB sorption can be evaluated using Equation (1):

$$\%\text{sorption} = \frac{(C_0 - C_e) \cdot 100}{C_e} \tag{1}$$

where C_0 and C_e are the initial and equilibrium concentrations ($mg{\cdot}L^{-1}$).

The amount of MB adsorbed at equilibrium was calculated using Equation (2):

$$q_e = \frac{(C_0 - C_e) \times V}{1000 \cdot m} \tag{2}$$

where C_0 and C_e are the initial and equilibrium concentrations ($mg{\cdot}L^{-1}$),

m the mass of sorbent (g), and
V the solution volume (ml).

Influence of pH

The pH dependence of MB adsorption by RH-1 and RH-2 was determined over the pH range 1 to 12, using a SevenCompact pH-meter (Mettler Toledo, Switzerland) and appropriate buffer solutions:

Water Practice & Technology Vol 16 No 2
doi: 10.2166/wpt.2020.117

pH 1 and 2 KCl/HCl;
pH 3 and 4 $KHC_8H_4O_4$/HCl;
pH 5 and 6 $KHC_8H_4O_4$/NaOH;
pH 8 and 9 Borax/HCl);
pH 10 and 11 Borax/NaOH); and
pH 12 KCl/NaOH).

100 mg samples were suspended by stirring in 10 ml of the relevant buffer solution and 1 ml of MB at 1,500 mg-MB L^{-1}. Stirring continued for 1 hour.

Point of zero charge

The point of zero charge of RH-1 and RH-2 was determined by the solid addition method (Vieira *et al.* 2009). 20.0 ml aliquots of solution were transferred to 100 ml conical flasks with the initial pH (pH_0) varying from 1 to 12. The initial pH was corrected in each case, where necessary, by adding 0.10 mol L^{-1} of either hydrochloric acid or sodium hydroxide. The solution pH_0 was then measured accurately and 0.10 g of RH-1 or RH-2 was added to each flask, which was securely capped immediately. The suspensions were mixed in a Unimax 1,010 (Heidolph, Germany) shaker for 24 hours and the supernatants' final pH values (pH_f) measured.

The difference between the initial and final pH values, $\Delta pH = pH_0 - pH_f$, was plotted against pH_0 and the point of intersection of the resulting null Δ pH corresponds to the point of zero charge, pH_{PZC}.

Ratio of sample weight to solution volume (S:V)

Samples weighing 1; 0.1; 0.04; 0.05 and 0.025 g were placed in 50 ml conical flasks, corresponding to the ratio of the sample mass to the solution volume (S:V) 1:10, 1:100, 1:250, 1:500 1:1,000, and 10 ml of MB solution was added (3.2 and 5.1 mg-MB L^{-1}). After 60 minutes, the solution and sample were separated by centrifugation. The residual MB content was determined as described in section 2.3, and the removal efficiency and amount of MB adsorbed using Equations (1) and (2).

Water suspension pH measurement

The water suspension pH was measured using 1; 0.1; 0.04; 0.05 and 0.025 g samples in conical flasks to which distilled water was added. The closed flasks were shaken for 30 minutes, after which the flask contents were centrifuged for 15 minutes. The pH of the medium was then measured.

Adsorption kinetics

The time needed to establish equilibrium was determined over periods of 1, 3, 5, 10, 15, 30, 60, 90 and 180 minutes at temperatures of 298 and 318 K.

Two kinetic models were used in the analysis (Janos *et al.* 2003): pseudo-first (Lagergren model) and pseudo-second order. Their respective integral equations are:

$$\ln(q_e - q) = \ln q_e - k_1 \cdot t \tag{3}$$

$$\frac{t}{q} = \frac{1}{k_2 \times q_e^2} + \frac{1}{q_e \times t} \tag{4}$$

where q is the amount of MB adsorbed at time t (mmol g^{-1});

q_e is the amount of MB adsorbed at equilibrium (mmol g^{-1});
k_1 is the sorption rate constant for the pseudo-first order model; and
k_2 is the sorption rate constant for the pseudo-second order model.

Water Practice & Technology Vol 16 No 2
doi: 10.2166/wpt.2020.117

Thermodynamics

Thermodynamic parameters including standard free energy change (ΔG^0, kJ mol^{-1}), enthalpy change (ΔH^0, kJ mol^{-1}) and entropy change (ΔS^0, J mol^{-1} K^{-1}) were determined using the van't Hoff equation as expressed in Equations (5) and (6) (Frolov 1988):

$$\ln K_d = -\frac{\Delta H}{RT} + \frac{\Delta S}{R} \tag{5}$$

$$\Delta G = \Delta H - T\Delta S \tag{6}$$

where K_d is the standard thermodynamic equilibrium defined by C_{ad}/C_e, in which C_{ad} (mg L^{-1}) is on the solid adsorbent and C_e (mg L^{-1}) is in the solution;

T is the absolute temperature, K; and
R is the universal gas constant (8.314 J mol^{-1} K^{-1}).

Adsorption equilibrium

The equilibrium sorption isotherm expresses the specific relationship between the sorbate concentration and its degree of accumulation on the sorbent surface at a constant temperature of 298 K. The MB sorption isotherm was developed using the separate portions method at different initial concentrations, ranging from 0.09 to 5.25 mmol-MB L^{-1}.

Different isotherm models were used to help to understand the nature of the adsorbate/adsorbent interactions – Freundlich (7), Langmuir (8), and Dubinin–Astakhov (9) (Keltsev 1984).

$$q_e = k_f C_e^{\frac{1}{n}} \tag{7}$$

where q_e is the sorbed concentration on the sorbent surface (mmol•g^{-1});

C_e is the equilibrium concentration in solution (mmol L^{-1});
k_f is the Freundlich constant; and
n is a constant.

$$q_e = q_0 \frac{kC_e}{1 + kC_e} \tag{8}$$

where q_e is the sorbed concentration on the sorbent surface (mmol•g^{-1});
C_e is the equilibrium concentration in solution (mmol L^{-1});
k is the Langmuir constant; and
q_0 is the monolayer adsorption capacity (mmol•g^{-1}).

$$q_e = q_m e^{-k\left(RT \cdot \ln \frac{C_s}{C_e}\right)^n} \tag{9}$$

where q_e is the sorbed concentration on the sorbent surface (mmol•g^{-1});
C_e is the equilibrium concentration in solution (mmol L^{-1});
q_m is the theoretical monolayer sorption capacity (mmol•g^{-1});
k is a constant;
R is the universal gas constant (8.314 J mol^{-1} K^{-1});
T is the absolute temperature, (K);
C_s is the limit of solubility (mmol L^{-1}); and
n – 1,2…6.

Water Practice & Technology Vol 16 No 2
doi: 10.2166/wpt.2020.117

RESULTS AND DISCUSSION

Adsorbent characterization

The SiO_2 content of RH-1 is 92.7%. Acid pre-treatment before oxidative roasting leads to the production of ash with a high SiO_2 content – 97.6%. The samples obtained contained traces of carbon, and alkali and alkaline earth metals, the amount depending on the sample's preliminary treatment (Table 1).

Table 1 | Sample composition (%)

Sample	SiO_2	Na_2O	CaO	MgO	Al_2O_3	MnO	Fe_2O_3	C
RH-1	92.7	0.05	0.55	0.71	0.03	0.15	0.10	2.00
RH-2	97.6	0.25	0.10	0.17	0.08	0.01	0.06	0.01

The IR spectroscopy showed that the structures of RH-1 and RH-2 are similar. In the spectra, the absorption bands correspond to the deformation (469 to 471 cm^{-1}) and stretching (symmetric and asymmetric) vibrations (804 to 806 cm^{-1} and 1,103 cm^{-1}) of the Si-O-Si siloxane bonds. The absorption bands at ~1,650 and ~3,400 cm^{-1} indicate the presence of OH groups. XRF analysis showed that RH-1 and RH-2 are in an X-ray amorphous state (Zemnukhova *et al.* 2014).

Effect of reaction pH on MB adsorption

Figure 1 shows curves of the changes in MB adsorption versus pH of the aqueous suspensions of RH-1 and RH-2.

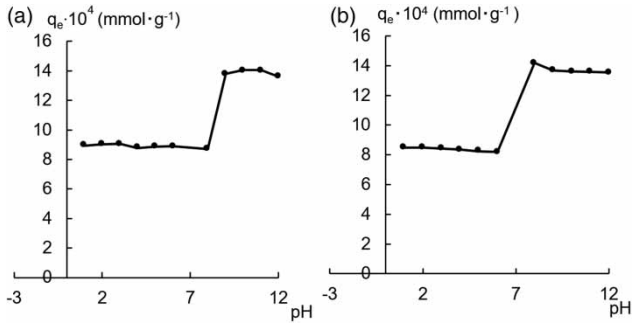

Figure 1 | Effect of pH on MB adsorption on (a) – RH-1, (b) – RH-2.

As can be seen, MB adsorption is minimal for RH-1 over the pH range 1 to 8 (Figure 1(a)), and for RH-2 from pH 1 to 6 (Figure 1(b)). When the medium becomes more alkaline (pH 9 for RH-1 and pH 8 for RH-2), adsorption increases sharply.

An important characteristic of the adsorbent is the zero charge point (pH_{PZC}) – that is, the pH at which the adsorbent surface has zero electric charge (Figure 2). At pH values below pH_{PZC}, the surface is charged positively, above it, negatively charged (Ghanizadeh & Asgari 2011; Van *et al.* 2018).

The surfaces of RH-1 and RH-2 carry proton-donating Bronsted acid centers (pKa +6.4) and proton-accepting Bronsted basic centers (pKa +7.15, +10.0), due to traces of alkaline earth metals (Table 1). On the surface of RH-1, there are more proton-acceptor Bronsted bases than on RH-2 due to the latter's higher impurity content (Arefieva *et al.* 2020). As a result, the surface of RH-1 remains positive up to pH 9.89 (Figure 2(a)), and RH-2 up to pH 6.01 (Figure 2(b)). Above pH_{PZC}, OH groups are fixed on the sample surfaces.

Water Practice & Technology Vol 16 No 2
doi: 10.2166/wpt.2020.117

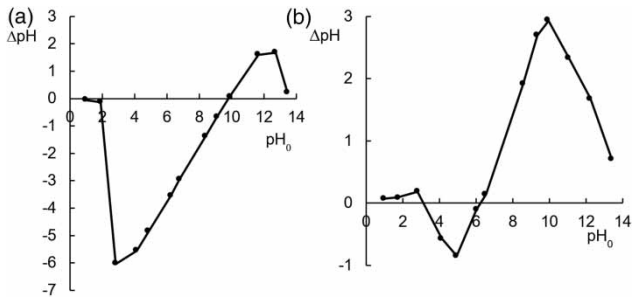

Figure 2 | Point of zero charge at 25 °C: (a) – RH-1, (b) – RH-2.

Based on the above:

At pH <3.8, the content of the undissociated form of MB increases, while that of the cationic form of MB^+ decreases.
At pH 3.8, MB is present in solution in two forms.
At pH > 3.8, MB's cationic character increases.
At pH >6, the predominant form becomes MB^+ (Abdelali *et al.* 2019).

It is also noted that the surface of RH-1 becomes negatively charged at pH > 10 and of RH-2 at pH >6 (Figure 2). Thus, the low adsorption rates in an acidic medium can be explained by a weak interaction between the molecular form of MB and the positively charged active centers RH-1 and RH-2, while electrostatic repulsion arises between the MB^+ and the surfaces. In an alkaline medium, electrostatic interaction occurs between the cationic form of MB^+ and the negatively charged silicon-containing surfaces.

S:V ratio effect on MB adsorption

As Figure 3(a) and 3(b) show, the MB adsorption efficiency increases for RH-1 and decreases for RH-2, with increased adsorbent mass. As RH-1's mass increases in solution, the pH rises (Figure 4(a)), leading to an increase in adsorption of the cationic form of MB. An increase in the mass of RH-2 lowers the solution pH (Figure 4(b)). In an acidic medium (see Section 3.2) MB adsorption is reduced by repulsion between the positively charged dye and the sorbent's protonated surface.

MB's proportional adsorption onto RH-1 and RH-2 decreases with increasing adsorbent mass (Figure 3(c) and 3(d)). This arises because, while the amount of adsorbent in the dye solution is low, MB molecules can reach the sorbent surface easily. An increase in adsorbent mass increases the number of adsorption centers but access to them can be blocked. A large amount of adsorbent also leads to particle agglomeration and a decrease in the total adsorption surface, and, consequently, a decrease in adsorption activity (Tamimi *et al.* 2018).

Analysis shows (Figure 3(a) and 3(b)) that at an S:V ratio of 1: 250, for both RH-1 and RH-2, the MB absorption efficiency is sufficiently high (86 and 97%, respectively; initial concentration 5.1 mg-MB L^{-1}) and adsorption activity (~1 mg g^{-1}). Because of that, this S:V ratio was used in further studies.

Adsorption kinetic and thermodynamics studies

The kinetic curves (Figure 5 – RH-1; Figure 6 – RH-2) show that the sorption equilibrium ~ 98% is reached 15 minutes after sorption starts – that is, this is sufficient time for MB absorption from aqueous solution. Analysis of the time dependence at 298 K using the known models (Soldatkina & Sagaydak 2010; Khokhlova *et al.* 2011; Romantsova *et al.* 2014) showed that MB sorption by RH-1 and RH-2 obeys the pseudo-second order model ($R^2 > 0.9$) (Table 2), indicating that the sorption

Water Practice & Technology Vol 16 No 2
doi: 10.2166/wpt.2020.117

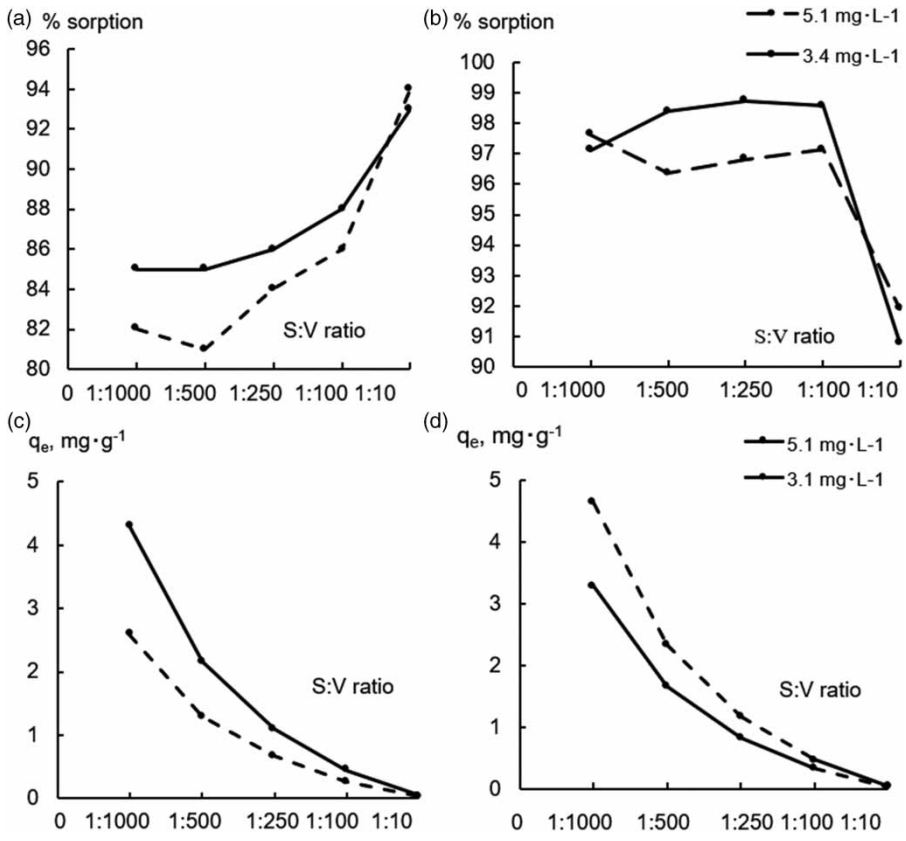

Figure 3 | MB removal efficiency (a), (b) and adsorbed amount at different S:V ratios: a, (c) – RH-1; b, (d) – RH-2.

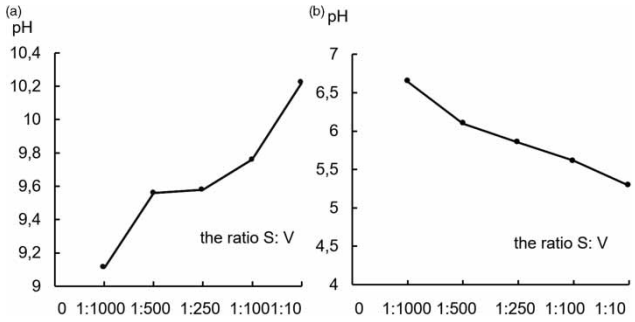

Figure 4 | Effect of S:V ratio on pH: (a) – RH-1, (b) – RH-2.

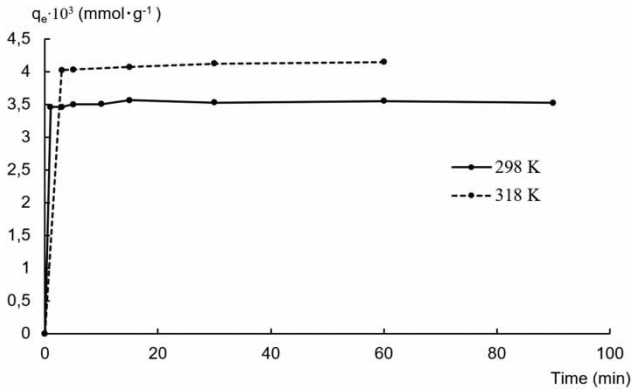

Figure 5 | Effects of contact time on RH-1 MB removal efficiency at different temperatures.

Water Practice & Technology Vol 16 No 2
doi: 10.2166/wpt.2020.117

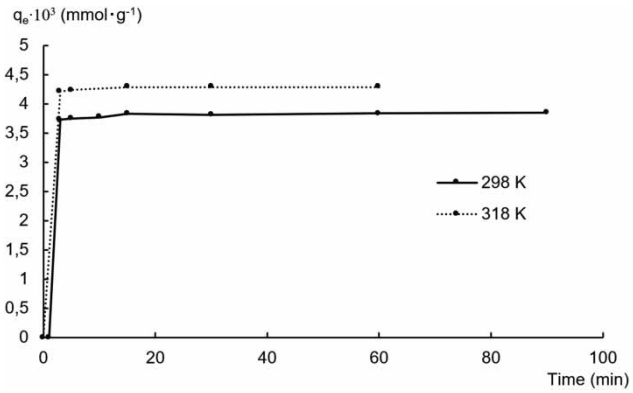

Figure 6 | Effects of contact time on RH-2 MB removal efficiency at different temperatures.

Table 2 | Kinetic model parameters

	Model					
	Pseudo-first order			Pseudo-second order		
Sample	R^2	$q_\infty \cdot 10^{-3}$ (mmol g^{-1})	k_1 (c^{-1})	R^2	$q_\infty \cdot 10^{-3}$ (mmol g^{-1})	k_2 (g·(mmol c)$^{-1}$)
RH-1	0.74	3.5	0.0016	1.00	3.50	120
RH-2	0.23	3.8	0.0017	1.00	3.8	212

process is determined by interaction between the sorbate (MB) and the samples' active centers. As the temperature rises to 318 K, MB sorption increases.

The change in Gibbs free energy, ΔG_{298}, is positive for both samples, which indicates that the process is not spontaneous. If the sample's ΔH value is negative, the process is exothermic, a positive change in entropy indicates molecular mobility in the layer upon adsorption from solution (Table 3).

Table 3 | Thermodynamic parameters of MB adsorption

Sample	ΔG_{298} (kJ mol^{-1})	ΔH (kJ mol^{-1})	ΔS (J/(mol·K)$^{-1}$
RH-1	20.61	−40.05	65.22
RH-2	7.46	−20.19	42.68

Equilibrium isotherms

Experimental MB-adsorption isotherms for silicon-containing RH products yield type I adsorption isotherms according to the BDDT classification (Brunauer, Deming, Deming, Teller) (Figure 7). This type of isotherm, characterized by the presence of an almost horizontal plateau, describes adsorption on many materials, including silica xerogels, oxides of titanium, aluminum, tin, etc, as well as carbon sorbents. Adsorption is usually limited because the pore sizes are very small and no more than one layer of molecules can form on their walls (Gregg & Sing 1982). Adsorption increases to a maximum associated with the presence of numerous adsorption sites and their availability. Then, as the concentration increases, the number of active sites available falls, and there are not enough of them to remove MB, so the adsorption capacity decreases.

The sorption isotherm was linearized in the coordinates of the Freundlich, Langmuir, and Dubinin-Astakhov equations. As it is assumed in the Langmuir model that adsorption occurs on the surface of a solid body consisting of active centers, and that RH-1 has a heterogeneous structure (SiO_2 content is

Water Practice & Technology Vol 16 No 2
doi: 10.2166/wpt.2020.117

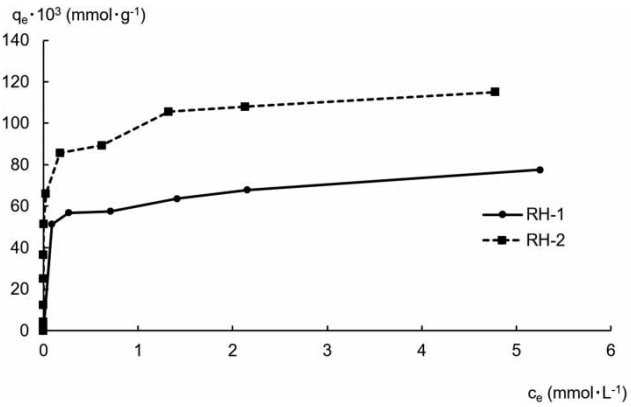

Figure 7 | Experimental MB adsorption isotherm.

92.7%), the model is difficult to apply to describe MB sorption. RH-2 is more homogeneous (SiO_2 97.6%) and the Langmuir equation can be used to determine the main parameters of the sorption process. As can be seen in Table 4, the adsorption isotherms for both samples are best described by the Freundlich and Dubinin-Astakhov equations. The Dubinin-Astakhov equation was logarithmized at $n = 1$–6, and the maximum approximation coefficients obtained were $n = 1$ for RH-1 and $= 6$ for RH-2.

The energy sorbent values were determined using the Dubinin-Astakhov equation. The values were low −RH-1 - 25.80 and RH-2 – 24.76 kJ mol^{-1}. It is also possible, using this equation, to calculate the total micropore volume – 0.038 cm^3 g^{-1} for RH-1 and 0.047 for RH-2.

Table 4 | Freundlich, Langmuir and Dubinin-Astakhov isotherm parameters for MB adsorption on RH-1 and RH-2 (T = 298 K)

	Sample	
Parameter	**RH-1**	**RH-2**
Freundlich equation		
Linearization equation	y = 0.096x – 2.761	y = 0.105x – 2.312
R^2	0.93	0.97
k_f, (mmol g^{-1}) · (L mmol^{-1})^n	0.06	0.09
1/n	0.10	0.10
Langmuir equation		
Linearization equation	y = 1.4467x – 20	y = 0.1309x + 9.794
R^2	0.66	0.84
S_{sp} (m^2 g^{-1})	–	122.94
q_∞ (mmol g^{-1})	–	0.10
k (g mmol^{-1})	–	0.01
R_L	–	0.99
Dubinin-Astakhov equation		
Linearization equation	y = −0.096x – 2.425	y = $-1\cdot10^{-6}$x – 2.217
R^2	0.93 ($n = 1$)	0.89 ($n = 6$)
k (mol kJ^{-1})	0.04	4.33
q_∞ (mmol g^{-1})	0.09	0.11
E (kJ mol^{-1})	25.80	24.76
W (cm^3 g^{-1})	0.038	0.047
S_{sp} (m^2 g^{-1}) 10^{-18}	106.52	131.21

Water Practice & Technology Vol 16 No 2
doi: 10.2166/wpt.2020.117

The experimental adsorption isotherm for RH-1 is close to those calculated using the Freundlich and Dubinin-Astakhov equations (Figure 8), that for RH-2 is closer to the Freundlich isotherm (Figure 9).

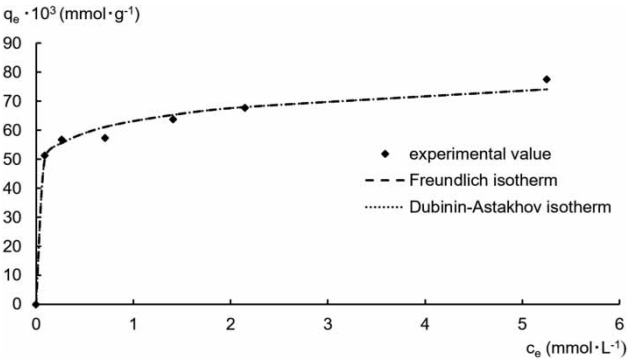

Figure 8 | MB adsorption isotherms on RH-1.

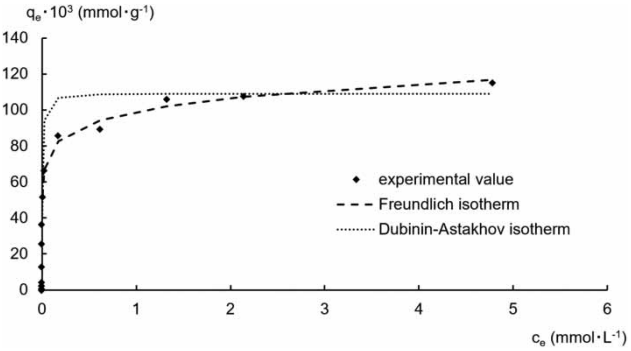

Figure 9 | MB adsorption isotherms on RH-2.

CONCLUSIONS

1. The study concerned the influence of conditions on methylene blue removal from aqueous solution by amorphous silicon dioxide obtained from rice husk by different processes (SiO_2 content 92.7 and 97.6%). It was established that the point of zero surface charge – RH-1 – pH 9.89; RH-2 – pH 6.01 – depends on the sorbent's composition and the number of Bronsted acid-base centers.
2. The study showed that the samples' methylene blue adsorption activity increases with increasing pH, reaching a maximum value above the point of zero charge. If the sorbent:solution ratio decreases, methylene blue adsorption decreases. It increases with increasing temperature.
3. For silicon-containing sorbents from rice husk, sorption equilibrium for methylene blue (~ 98%) is achieved in 15 minutes. The thermodynamic parameter values obtained ($\Delta G_{298} > 0, \Delta H < 0, \Delta S > 0$) indicate that the methylene blue adsorption process is exothermic and occurs with an increase in molecular mobility in the adsorption layer.
4. The methylene blue adsorption mechanism by rice husk-derived silicon-containing sorbents was also studied. In the concentration range 0 to 5.2 mmol L^{-1} the process is described by the Freundlich and Dubinin-Astakhov equations. Methylene blue adsorption is determined by both electrostatic interaction with active centers on the surface and the volumetric filling of the micropore adsorption space.

Water Practice & Technology Vol 16 No 2
doi: 10.2166/wpt.2020.117

DATA AVAILABILITY STATEMENT

All relevant data are included in the paper or its Supplementary Information.

REFERENCES

Abdelali, G., Charlotte, H., Abdelmalek, C., Réda, Y. A., Ammar, S. & Boubekeur, N. 2019 Adsorptive removal of methylene blue by low cost agricultural waste: Degla beida Dates Stones in a fixed-bed dynamic column. *Research Journal of Chemistry and Environment* **23**(1), 74–81.

Arefieva, O. D., Pirogovskaya, P. D., Panasenko, A. E., Kovekhova, A. V. & Zemnukhova, L. A. 2020 Acid-base properties of amorphous silicon dioxide from straw and rice husk. *Khimija Rastitel'nogo Syr'ja* (in press).

Balykin, V. P., Efremova, O. A. & Bulatov, A. V. 2004 Adsorption of methylene blue and methanyl yellow on a carbon surface. *Bulletin of Chelyabinsk State University* **4**(1), 46–57.

Corda, N. C. & Kini, M. S. 2018 A review on adsorption of cationic dyes using activated *Carbon*. *MATEC Web of Conferences* **144**, Art. 02022. https://doi.org/10.1051/matecconf/201814402022.

Djilani, C., Zaghdoudi, R., Djazi, F., Bouchekima, B., Lallam, A., Modarressi, A. & Rogalski, M. 2015 Adsorption of dyes on activated carbon prepared from apricot stones and commercial activated carbon. *Journal of the Taiwan Institute of Chemical Engineers* **53**, 112–121. https://doi.org/10.1016/j.jtice.2015.02.025.

Dŏgan, M., Alkan, M., Türkyilmaz, A. & Özdemir, Y. 2004 Kinetics and mechanism of removal of methylene blue by adsorption onto perlite. *Journal of Hazardous Materials* **109**(1–3), 141–148. doi:10.1016/j.jhazmat.2004.03.003.

Dŏgan, M., Abak, H. & Alkan, M. 2009 Adsorption of methylene blue onto hazelnut shell: kinetics, mechanism and activation parameters. *Journal of Hazardous Materials* **164**(1), 172–181. doi:10.1016/j.jhazmat.2008.07.155.

Frolov, Y. G. 1988 *Course of Colloid Chemistry. Surface Phenomena and Dispersed Systems*. Chemistry, Moscow.

Ghanizadeh, G. & Asgari, G. 2011 Adsorption kinetics and isotherm of methylene blue and its removal from aqueous solution using bone charcoal. *Reaction Kinetics, Mechanisms and Catalysis* **102**, 127–142. doi:10.1007/s11144-010-0247-2.

GOST 9428-73. 1993 *Reagents. Silicon Dioxide. Specifications*. Publishing House of Standards, Moscow.

Gregg, S. J. & Sing, K. S. W. 1982 *Adsorption, Surface Area and Porosity*. Academic Press, London, UK.

Janos, P., Buchtova, H. & Ryznarova, M. 2003 Sorption of Dye from Aqueous Solution onto Fly Ash. *Water Research* **37**(20), 4938–4944. doi:10.1016/j.watres.2003.08.011.

Jawad, A. H., Waheeb, A. S., Rashid, R. A., Nawawi, W. I. & Yousif, E. 2018 Equilibrium isotherms, kinetics, and thermodynamics studies of methylene blue adsorption on pomegranate (*Punica granatum*) peels as a natural low-cost biosorbent. *Desalination and Water Treatment* **105**, 322–331. doi:10.5004/dwt.2018.22021.

Jia, P., Tan, H., Liu, K. & Gao, W. 2017 Adsorption behavior of methylene blue by bone char. *International Journal of Modern Physics B* **31**, Art. 1744099. doi:10.1142/S0217979217440994.

Keltsev, N. V. 1984 *Fundamentals of Adsorption Technology*. Institute of Chemistry, Moscow.

Khokhlova, T. D., Vlasenko, E. V., Hryashchikova, D. N., Lanin, S. N. & Smirnov, V. V. 2011 Adsorption and gas chromatographic properties of silochromes modified with silver. Bulletin of Moscow University. Series 2. *Chemistry* **52**(2), 102–107.

Lakkaboyana, S. K., Khantong, S., Asmel, N. K., Yuzir, A. & Yaacob, W. Z. W. 2019 Synthesis of copper oxide nanowires-activated carbon ((AC@ CuO-NWs)) and applied for removal methylene blue from aqueous solution: kinetics, isotherms, and thermodynamics. *Journal of Inorganic and Organometallic Polymers and Materials* **29**, 1658–1668. https://doi.org/10.1007/s10904-019-01128-w.

Liu, Y., Zhao, X., Li, J., Ma, D. & Han, R. 2012 Characterization of bio-char from pyrolysis of wheat straw and its evaluation on methylene blue adsorption. *Desalination and Water Treatment* **46**(1–3), 115–123. http://dx.doi.org/10.1080/19443994.2012.677408.

Mouni, L., Belkhiri, L., Bollinger, J.-C., Bouzaza, A., Assadi, A., Tirri, A., Dahmoune, F., Madani, K. & Remini, H. 2018 Removal of methylene blue from aqueous solutions by adsorption on kaolin: kinetic and equilibrium studies. *Applied Clay Science* **153**, 38–45. https://doi.org/10.1016/j.clay.2017.11.034.

Mulugeta, M. & Lelisa, B. 2014 Removal of methylene blue (Mb) dye from aqueous solution by bioadsorption onto untreated *Parthenium hystrophorous* weed. *Modern Chemistry and Applications* **2**(4), Art. 1000146. doi:10.4172/2329-6798.1000146.

P'yanova, L. G., Likholobov, V. A., Drozdetskaya, M. S., Sedanova, A. V., Kornienko, N. V. & Gerunova, L. K. 2017 Adsorption of methylene blue and metanil yellow dyes by modified carbon sorbents. *Russian Journal of Applied Chemistry* **90**(12), 2004–2008.

Rafatullah, M., Sulaiman, O., Hashim, R. & Ahmad, A. 2010 Adsorption of methylene blue on low-cost adsorbents: a review. *Journal of Hazardous Materials* **177**(1–3), 70–80. doi:10.1016/j.jhazmat.2009.12.047.

Romantsova, I. V., Burakov, A. E. & Kucherova, A. E. 2014 Study of the kinetics of the process of liquid-phase adsorption of organic substances on hybrid nanostructured carbon sorbents. *Izvestia of the Samara Scientific Center of the Russian Academy of Sciences* **16**, 611–614. 4(3).

Water Practice & Technology Vol 16 No 2
doi: 10.2166/wpt.2020.117

Selyutin, A. A., Kolonitsky, P. D., Sukhodolov, N. G., Schreiner, E. V., Krasnov, N. V. & Podolskaya, E. P. 2013 Synthesis and characterization of nanoregular sorbents based on zirconium oxide. *Scientific Instrumentation* **23**(1), 115–122.

Sergienko, V. I., Zemnukhova, L. A., Egorov, A. G., Shkorina, E. D. & Vasilyuk, N. S. 2004 Renewable sources of chemical raw materials: complex processing of waste from rice and buckwheat production. *Russian Chemical Journal (Journal of the Russian Chemical Society Named After D.I. Mendeleev)* **48**(3), 116–124.

Singh, H., Chauhan, G., Jain, A. K. & Sharma, S. K. 2017 Adsorptive potential of agricultural wastes for removal of dyes from aqueous solutions. *Journal of Environmental Chemical Engineering* **5**, 122–135. http://dx.doi.org/10.1016/j.jece.2016.11.030.

Soldatkina, L. M. & Sagaydak, E. V. 2010 Kinetics of adsorption of water-soluble dyes on active coals. *Chemistry and Technology of Water* **32**(4), 388–398.

Soldatkina, L. & Zavrichko, M. 2018 Equilibrium, kinetic, and thermodynamic studies of anionic dyes adsorption on corn stalks modified by cetylpyridinium bromide. *Colloids and Interfaces* **3**(1), Art. 4. https://doi.org/10.3390/colloids3010004.

Tamimi, M, Bougdour, N., Alahaine, S., Sennaoui, A. & Assabbane, A. 2018 A study of the remove cationic and anionic dyes in aqueous solution by a new natural clay. *International Journal of Engineering Technologies and Management Research* **5**(10), 64–74. doi:10.5281/zenodo.1486263.

Van, H. T., Nguyen, T. M. P., Thao, V. T., Vu, X. H., Nguyen, T. V. & Nguyen, L. H. 2018 Applying activated carbon derived from coconut shell loaded by silver nanoparticles to remove methylene blue in aqueous solution. *Water Air and Soil Pollution* **229**, Art. 393. https://doi.org/10.1007/s11270-018-4043-3.

Vieira, A. P., Santana, S. A. A., Bezerra, C. W. B., Silva, H. A. S., Chaves, J. A. P., de Melo, J. C. P., da Silva Filho, E. C. & Airoldi, C. 2009 Kinetics and thermodynamics of textile dye adsorption from aqueous solutions using babassu coconut mesocarp. *Journal of Hazardous Materials* **166**, 1272–1278. doi:10.1016/j.jhazmat.2008.12.043.

Zemnukhova, L. A., Panasenko, A. E., Fedorishcheva, G. A., Maiorov, V. Y., Tsoi, E. A., Shapkin, N. P. & Artem'yanov, A. P. 2014 Composition and structure of amorphous silica produced from rice husk and straw. *Inorganic Materials* **50**(1), 75–81. doi:10.7868/S0002337X14010205.

First received 8 October 2020; accepted in revised form 5 December 2020. Available online 14 December 2020